Electronic Supplementary Information

A quinoxaline−naphthaldehyde conjugate for colorimetric determination of copper ion

Sutapa Sahu[1], Yeasin Sikdar[1,2], Riya Bag [1], Michael G. B. Drew [3], José P. Cerón-Carrasco [4,*] and Sanchita Goswami[1,*]

[1] Department of Chemistry, University of Calcutta, 92, A.P.C. Road, Kolkata 700009, India; sutapa.sahu11@gmail.com (S.S.); y.sikdar@gmail.com (Y.S.); riyabag.chem@gmail.com (R.B.)

[2] Department of Chemistry, The Bhawanipur Education Society College, 5, Lala Lajpat Rai Sarani, Kolkata 700020, India; y.sikdar@gmail.com (Y.S.)

[3] Department of Chemistry, University of Reading, Whiteknights, Reading RG6 6AD, UK

[4] Centro Universitario de la Defensa, Academia General del Aire, Universidad Politécnica de Cartagena, C/Coronel López Peña S/N, Santiago de La Ribera, 30720 Murcia, Spain

***** Correspondence: jose.ceron@cud.upct.es (J.P.C.-C.); sgchem@caluniv.ac.in (S.G.)

Contents of the Supporting Information

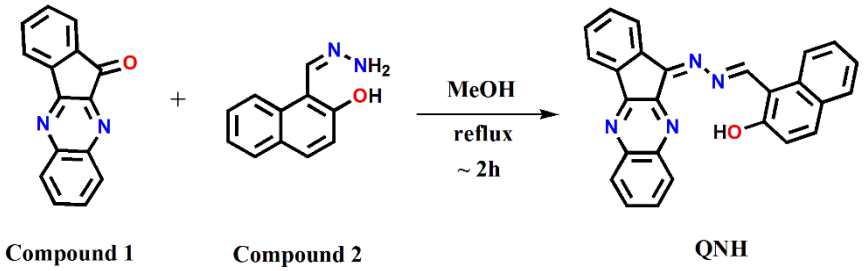

Scheme S1. Synthetic procedure of QNH**.**

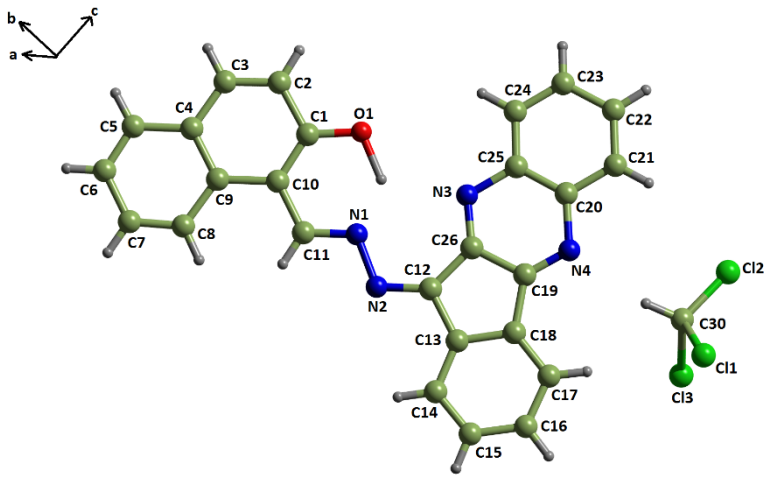

Figure S1. Molecular structure of QNH. Color code: C = pista green; N = blue; O = red; H= gray; Cl = bright green.

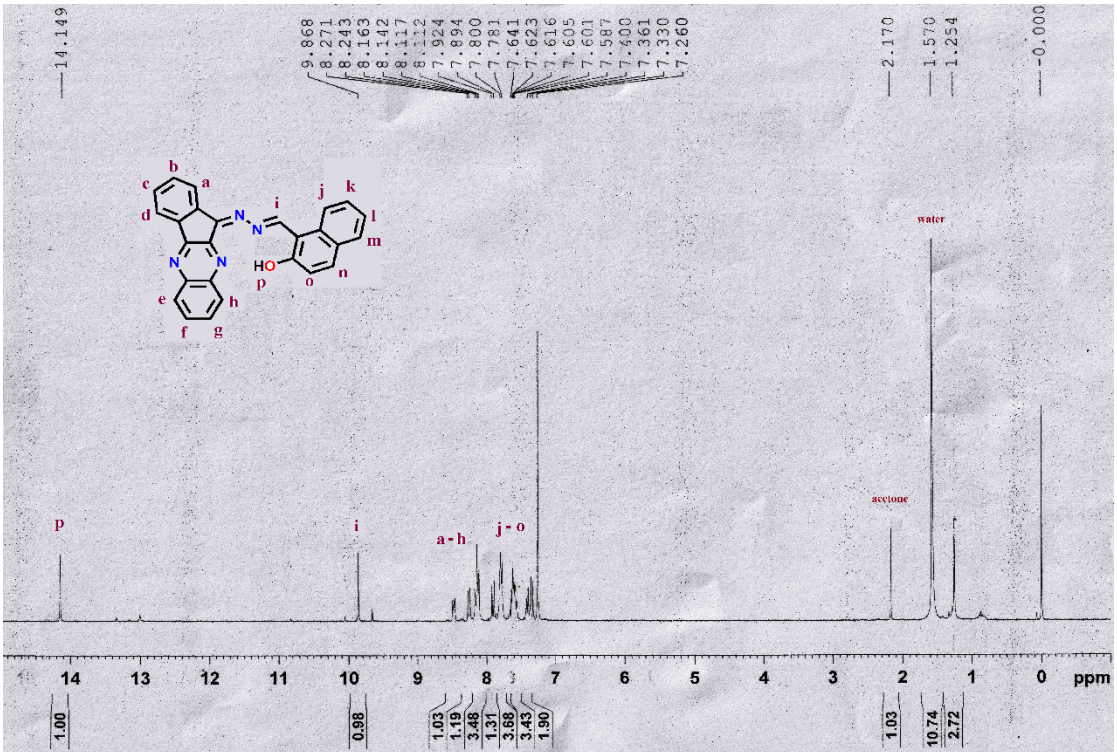

Figure S2. ^{1}H NMR spectrum of QNH in $CDCl_3$.

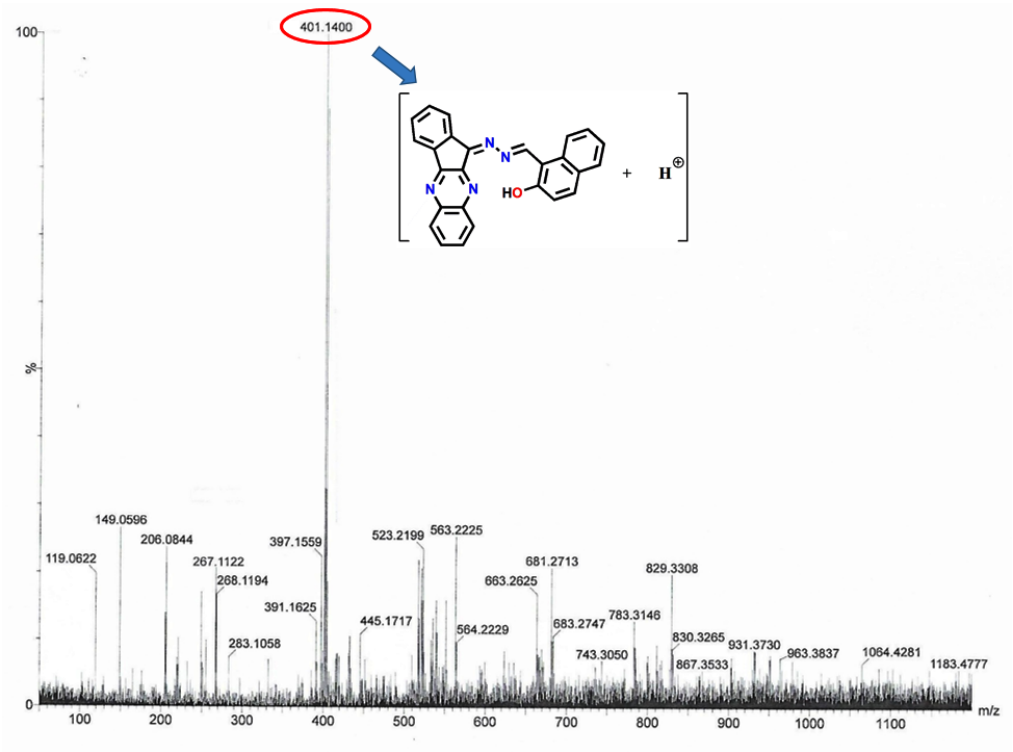

Figure S3. ESI–MS spectrum of QNH.

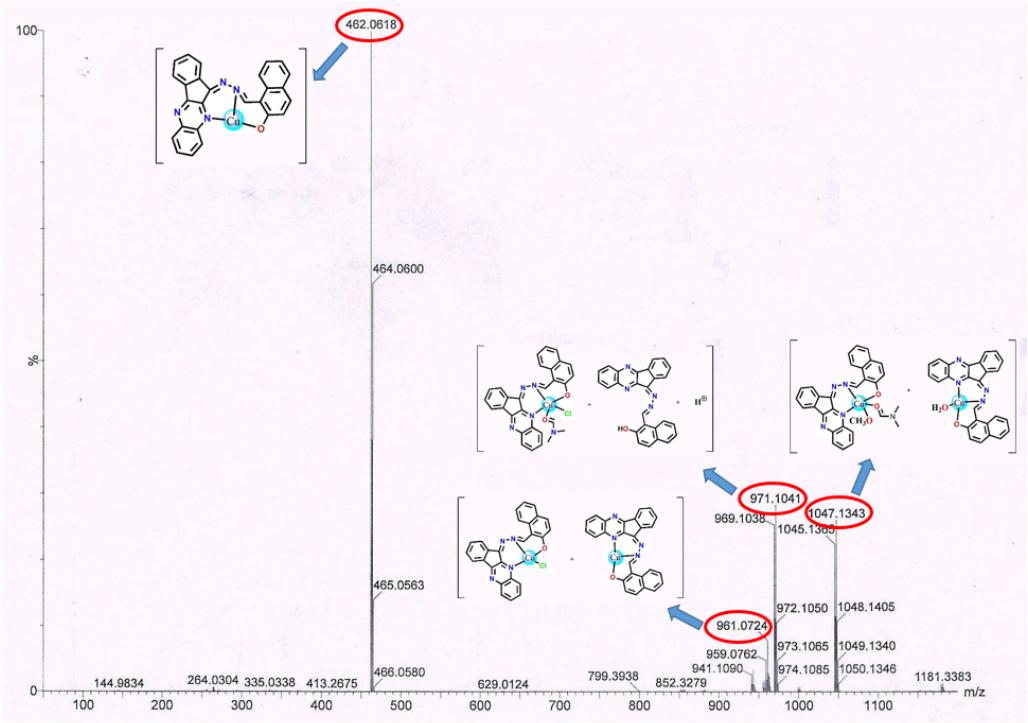

Figure S4. ESI–MS Spectrum of QNH + Cu^{2+} complex.

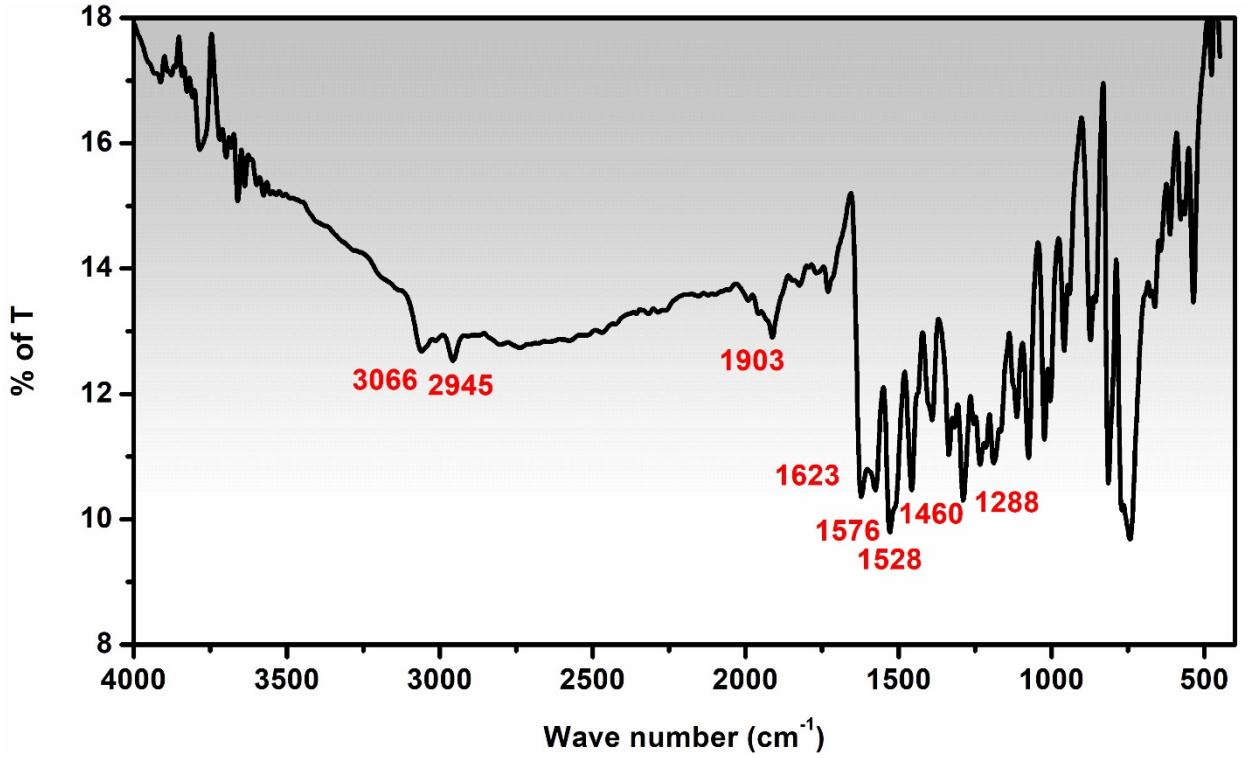

Figure S5. FT–IR Spectrum of QNH.

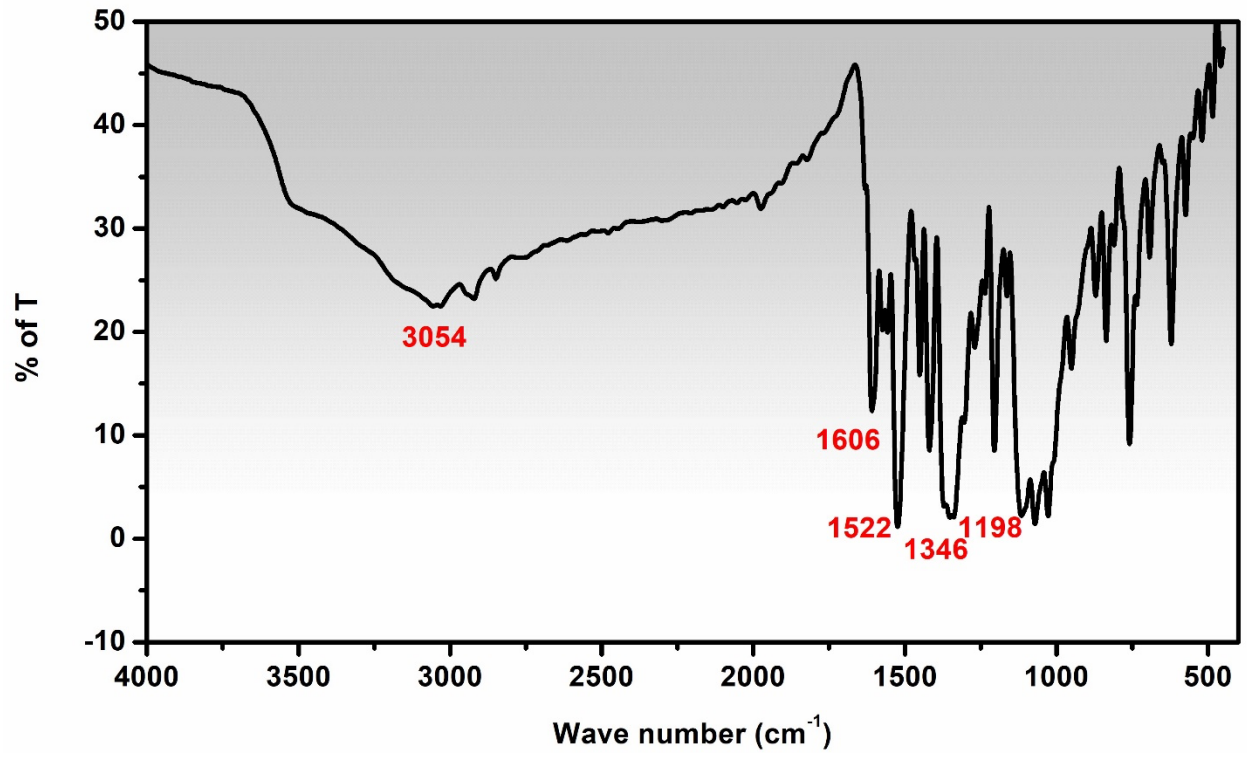

Figure S6. FT–IR Spectrum of QNH + Cu^{2+} complex

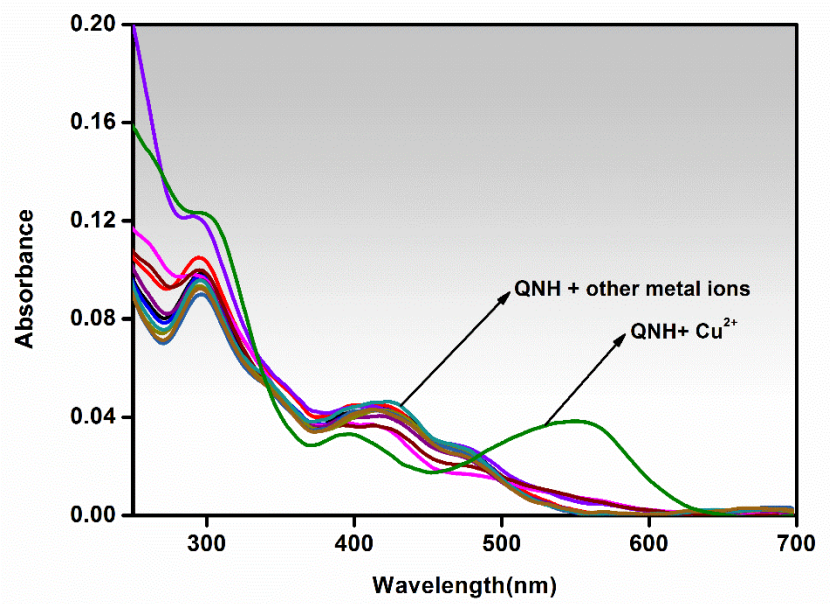

Figure S7. Absorbance spectra of QNH (10^{-5} M) in presence of 5 equiv. of various cations (Na^{+}, K^{+}, Ca^{2+}, Mg^{2+}, Hg^{2+}, Ni^{2+}, Fe^{3+}, Cu^{2+}, Co^{2+}, Cd^{2+}, Zn^{2+}, Mn^{2+}, Pb^{2+}, Al^{3+}, Cr^{3+}) in (3:7, v/v)HEPES buffer : acetonitrile medium.

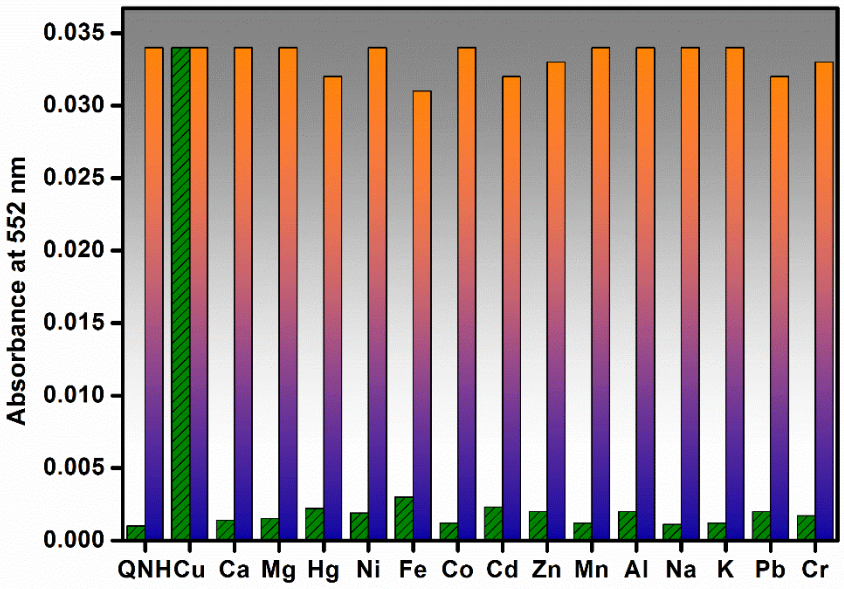

Figure S8. Absorption intensity of QNH (10^{-5} M) in the presence of 5 equiv. of different cations in absence of same equiv. of Cu^{2+} in solution [the green bar portion]. Absorption intensity of a mixture of **QNH** (10^{-5} M) with 5 equiv. of other cations followed by addition of 5 equiv. of Cu^{2+} to the solution (λ_{abs}=552nm) [the orange blue bar portion].

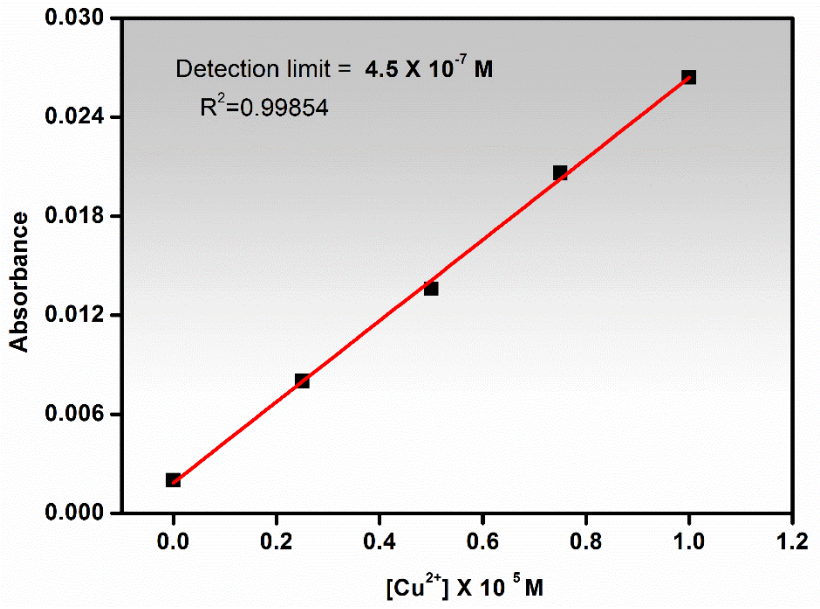

Figure S9. Determination of the detection limit of QNH in presence of Cu^{2+} in (3:7, v/v) HEPES buffer : acetonitrile medium at 552 nm.

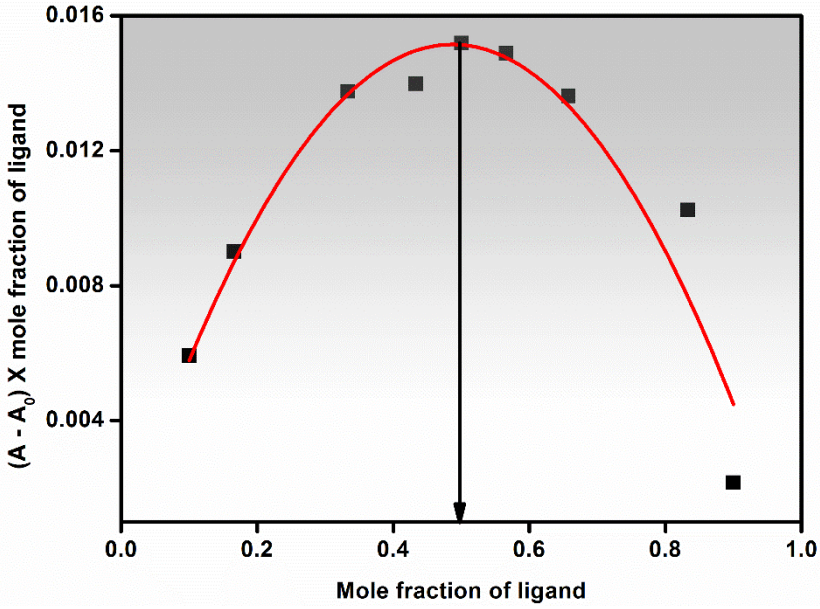

Figure S10. Job′s plot for the identification of stoichiometry using absorbance values at 552 nm.

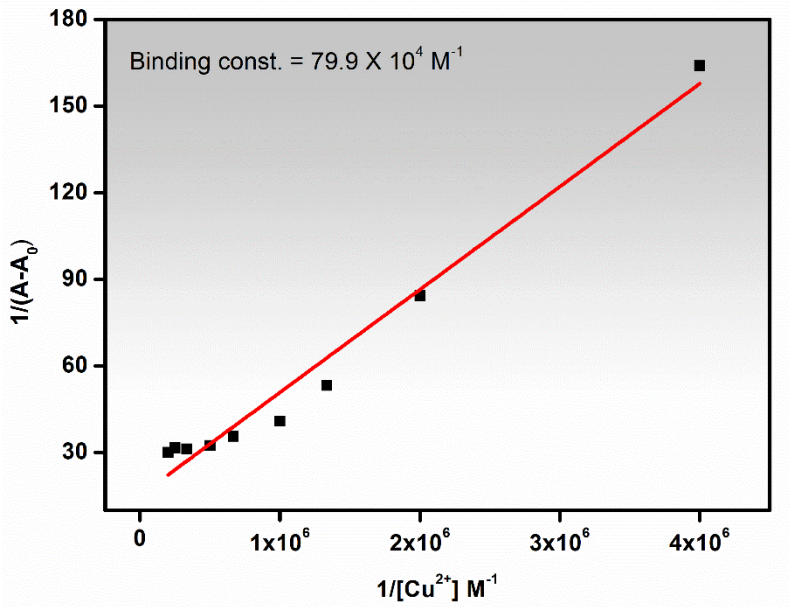

Figure S11. Benesi-Hildebrand plot for determination of binding constant of QNH with Cu^{2+}.

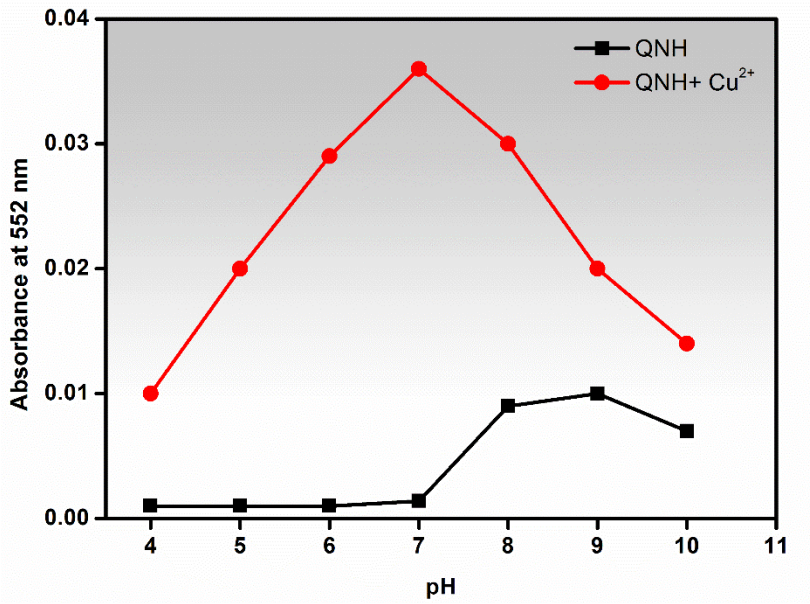

Figure S12. Absorbance of QNH in absence and in presence of Cu^{2+} at different pH values.

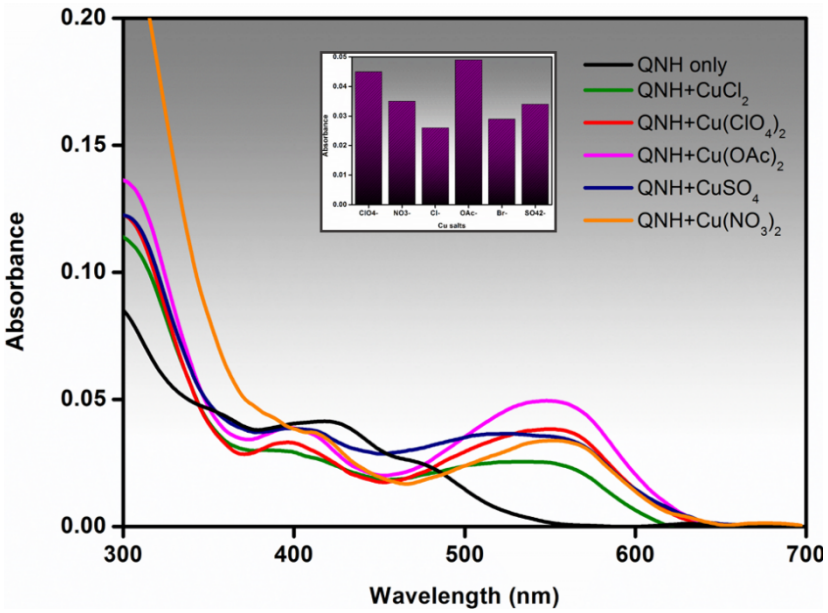

Figure S13. Absorbance spectra of QNH in present different anion Cu^{2+} of salts. (Inset: Bar plot of QNH in present different anion Cu^{2+} of salts)

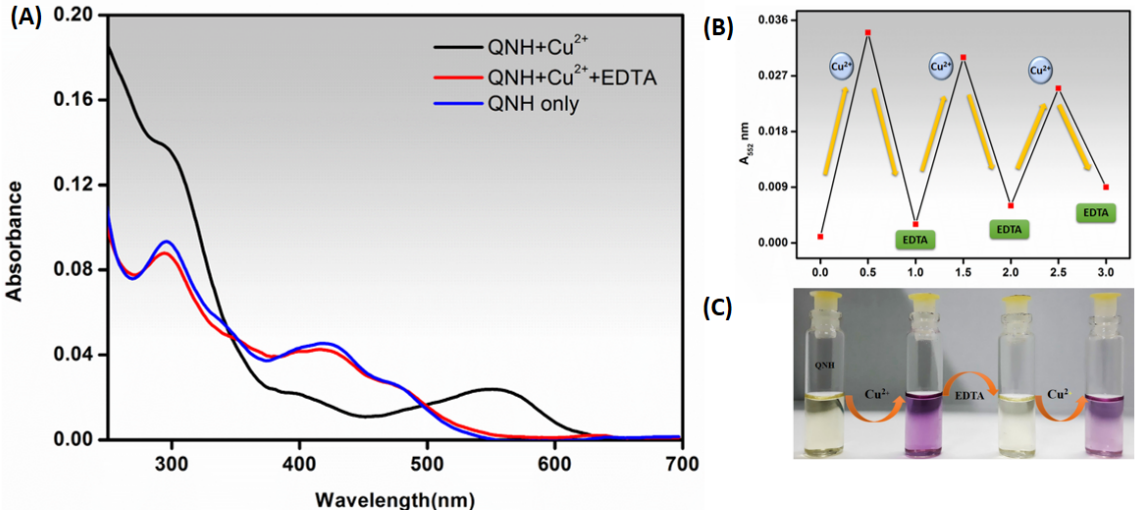

Figure S14. (A) Absorption spectrum of QNH shows reversibility towards Cu^{2+} in presence of EDTA in (3:7, v/v)HEPES buffer : acetonitrile medium. (B) The reversible colorimetric switch by alternate addition of $Cu^{2+}$and EDTA into the (3:7, v/v)HEPES buffer : acetonitrile medium. (C) Visual color change of **QNH** showing reversibility towards Cu^{2+} in presence of EDTA.

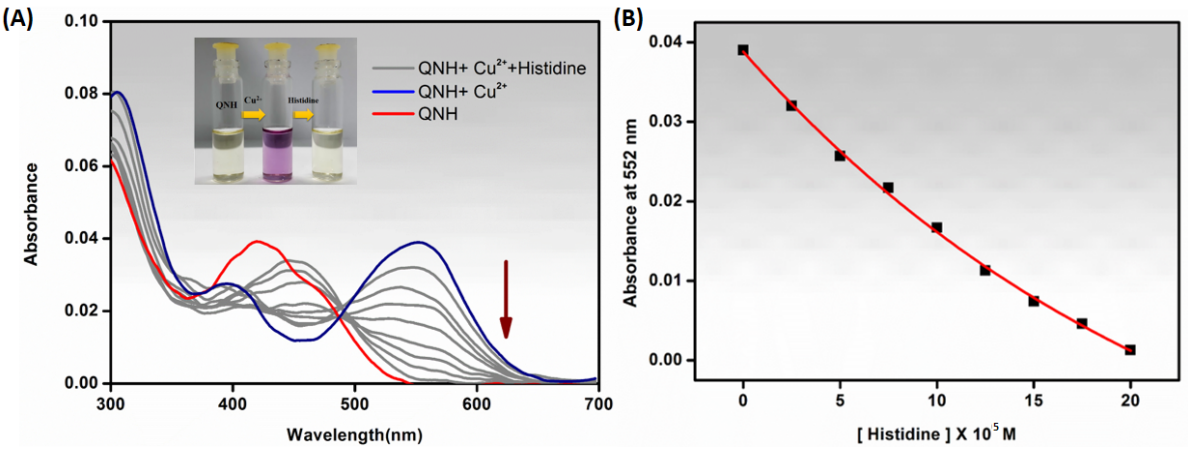

Figure S15. (A)UV–Vis titration of QNH–Cu^{2+} complex (10^{-5}M) in the presence of various concentration of Histidine. (Downward arrow indicates gradual decrease of absorption at 552 nm with increasing concentration of externally added Histidine) (Inset: Visual color change of QNH in presence of Cu^{2+} followed by histidine). (B)Absorbance of QNH–Cu^{2+} complex at 552 nm as a function of [Histidine]).

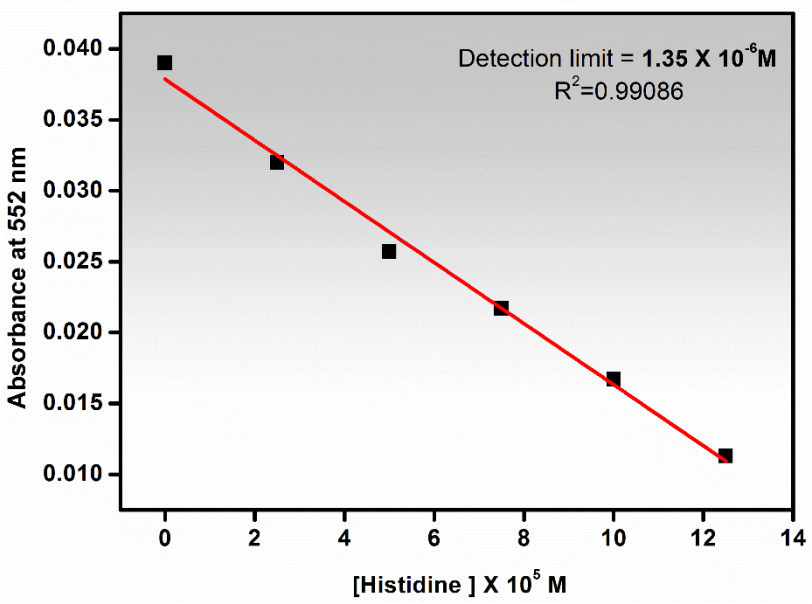

Figure S16. Determination of the detection limit of Histidine in (3:7 v/v)HEPES buffer : acetonitrile medium at 552 nm.

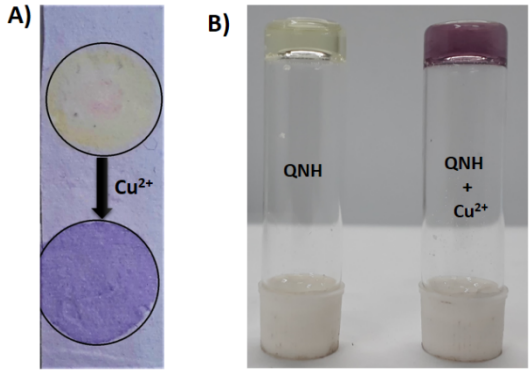

Figure S17. Visual change of QNH in presence of Cu^{2+} in A) paper strip and B)gel form.

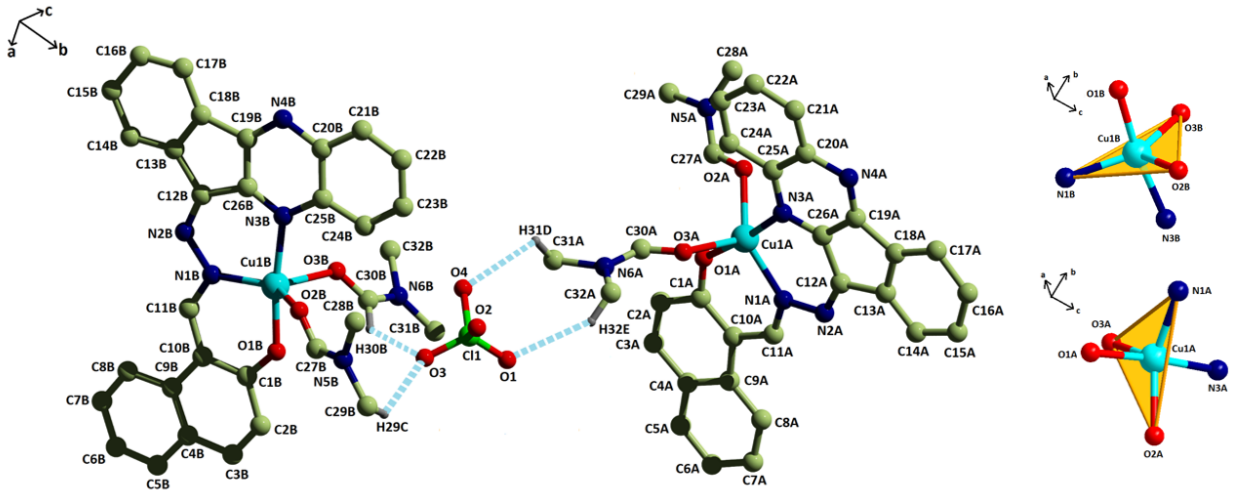

Figure S18. Crystal structure of QNH + Cu^{2+} metal complex. (Inset: The geometry of the two Cu centre of the complex in unit A and unit B). Color code: C = pista green; N = blue; O = red; H= gray; Cl = bright green; Cu = cyan.

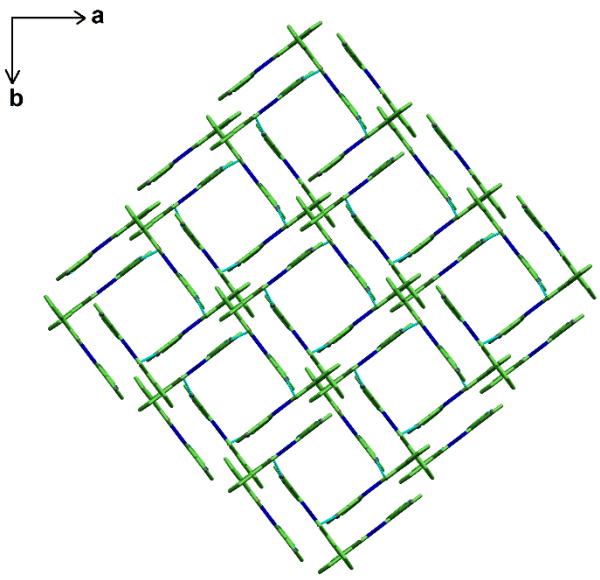

Figure S19. The supramolecular 2D packing diagram of the QNH showing the propagation via H–bonding and short ring–interactions, forms a 2D sheet like structure.

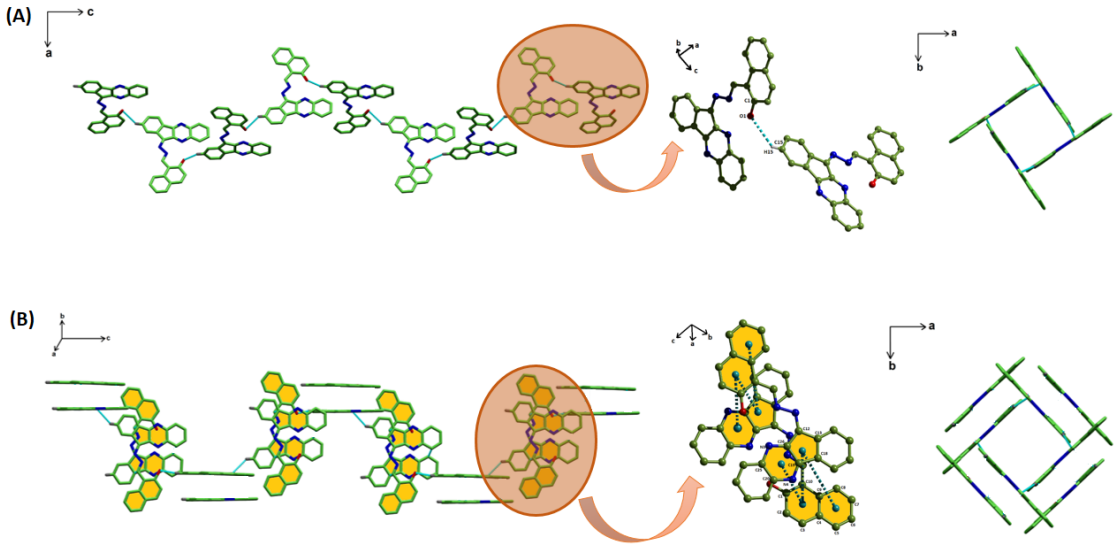

Figure S20. The supramolecular 1D packing diagram of QNH via (A)H–bonding interaction along b axis with enlarged version and c axis view of the interaction ; (B) short ring–interactions with enlarged version and c axis view of the interaction.

Table S1. Colorimetric Cu^{2+} sensing receptors found in the literature.

Ligand structure	Solvent	Detection limit (Absorption)	Ref.
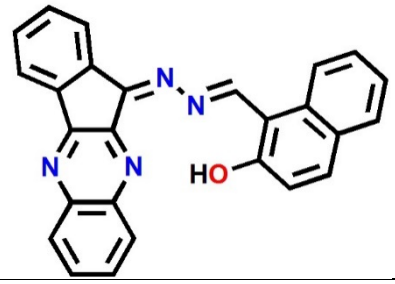	HEPES buffer : CH_3CN (3:7;v/v)	0.45 µM	This work
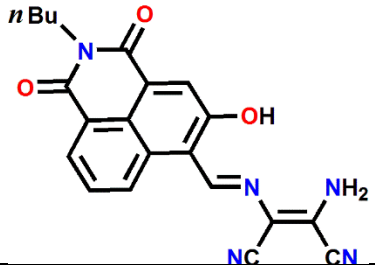	DMSO	1.6 µM	[1]
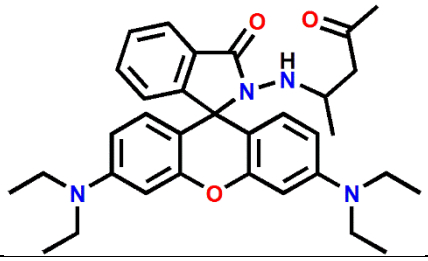	EtOH/ HEPES buffer (9:1; v/v)	2 µM	[2]
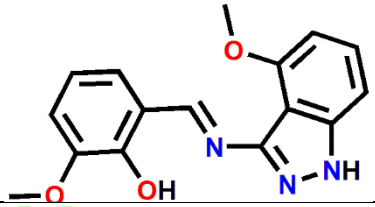	Bis-tris buffer/DMSO (7:3; v/v)	0.14 µM	[3]
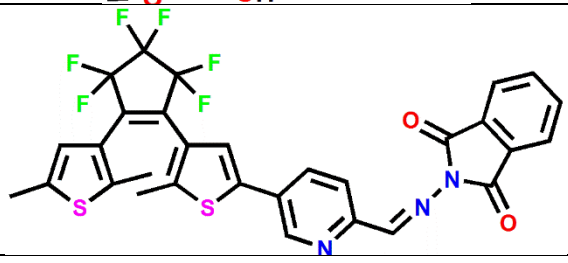	MeOH	0.041 µM	[4]

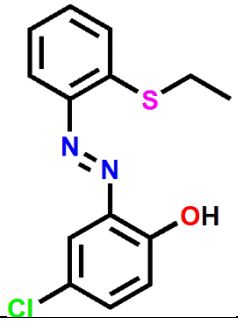	CH_3CN	0.062 µM	[5]
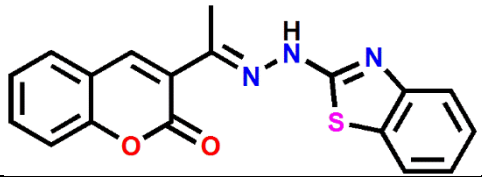	THF: water(9: 1; v/v)	1.54 µM	[6]
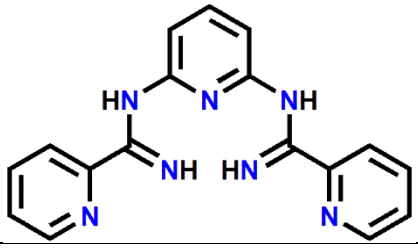	EtOH:H_2O (1:9;v/v)	3.49 µM	[7]
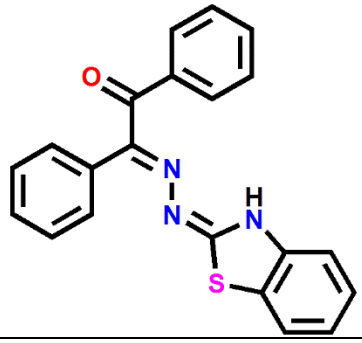	THF–HEPES buffer (9:1;v/v)	10 µM	[8]
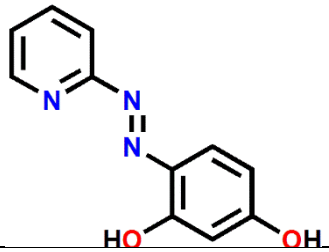	H_2O	0.031 µM	[9]

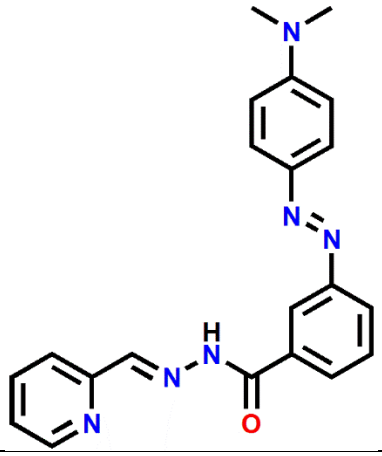	CH_3CN:HEPES buffer (1:1;v/v)	3.68 μM	[10]
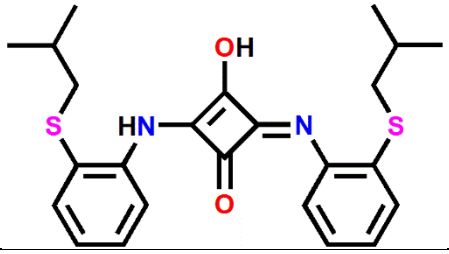	CH_3CN/H_2O (4:1;v/v)	8.06 μM	[11]

Table S2. The crystallographic data for QNH.

CCDC No	2156635
Chem. Formula	$2(C_{26}H_{16}N_4O)$, C H Cl_3
Formula weight	920.22
Crystal color, habit	Orange, rectangular
Temp (K)	296
λ[a]/ Å	0.71073
Crystal system	tetragonal
Space group	I 41/a
Unit cell dimensions	
a (Å)	16.455(2)
b(Å)	16.455(2)
c(Å)	33.088(9)
α(deg)	90

β (deg)	90
γ (deg)	90
Volume (Å^3), Z	8959(3),8
Density (mg m^{-3})	1.365
Absorption Coeff(mm^{-1})	0.258
F(000)	3792
Crystal size (mm)	0.19×0.17×0.12
θ range (deg)	1.3–23.7
Limiting indices	–18≤h≤17 –18≤k≤18 –35≤l≤37
Reflections collected	19954
Unique reflections [R_{int}]	3383(0.093)
Completeness to θ	98.5%(23.7)
Data/restraints/parameters	3383/0/319
GOOF on F^2	1.083
R_1[a], wR_2[b]values [I > 2σ(I)]	0.1034,0.3079
R_1[a],wR_2[b] values (all data)	0.1861,0.3480
Maximum, minimum residual peaks (e Å^{-3})	0.584, -0.400

[a]Graphitemonochromator [b]$R_1 = \Sigma(|F_o| - |F_c|)/\Sigma|F_o|$. [c]$wR_2 = \{\Sigma[w(|F_o|^2 - |F_c|^2)^2]/\Sigma[w(|F_o|^2)^2]\}^{1/2}$

Table S3. The crystallographic data for QNH + Cu^{2+}.

CCDC No	2156636
Chem. Formula	C_{32} H_{30} $Cl_{0.75}$ Cu N_6 $O_{6.50}$
Formula weight	692.75
Crystal color, habit	black bronze, rectangular cuboid
Temp (K)	296
λ[a]/ Å	0.71073
Crystal system	triclinic
Space group	*P -1*

Unit cell dimensions	
a (Å)	14.067(4)
b(Å)	15.587(4)
c(Å)	15.601(4)
α(deg)	106.091(7)
β (deg)	91.734(7)
γ (deg)	100.266(8)
Volume (Å^3), Z	3222.4(14),4
Density (mg m^{-3})	1.428
AbsorptionCoeff(mm^{-1})	0.795
F(000)	1431
Crystal size (mm)	0.20×0.17×0.11
θ range (deg)	1.36–24.9
Limiting indices	–13≤h≤16
	–18≤k≤18
	–18≤l≤18
Reflections collected	27051
Unique reflections [R_{int}]	11126(0.067)
Completeness to θ	99.7% (24.9)
Data/restraints/parameters	11126/0/838
GOOF on F^2	2.051
R_1[a], wR_2[b]values [I > 2σ(I)]	0.1842, 0.4651
R_1[a],wR_2[b] values (all data)	0.2217,0.5019
Maximum, minimum residual peaks (e Å^{-3})	3.32, -1.03

[a]Graphitemonochromator [b]$R_1 = \Sigma(|F_o| - |F_c|)/\Sigma|F_o|$. [c]$wR_2 = \{\Sigma[w(|F_o|^2 - |F_c|^2)^2]/\Sigma[w(|F_o|^2)^2]\}^{1/2}$

Table S4. Analysis of X–I···J (H bonding) interactions in QNH. (Bond lengths (Å), bond angles (°))

I	J	Distance(I···J)	X	∠X–I···J
O1	H15	2.65	C1	104°

Table S5. Analysis of short ring–interactions with Cg···Cg distances (Å) in QNH.

Cg···Cg	Cg···Cg distance (Å)	Slippage(Å)
Cg1···Cg3	3.7606(10)	1.382
Cg3···Cg1	3.7606(10)	1.333
Cg1···Cg4	3.9321(11)	1.824
Cg4···Cg1	3.9321(11)	1.741
Cg2···Cg4	3.5062(10)	0.327
Cg4···Cg2	3.5062(10)	0.406

Cg1: C12 C13 C18 C19 C26

Cg2: N3 C25 C20 N4 C19 C26

Cg3:C1 C2 C3 C4 C9 C10

Cg4:C4 C5 C6 C7 C8 C9

References

[1] I. J. Chang, M. G. Choi, Y. A. Jeong, S. H. Lee, S.-K. Chang, Tetrahedron Lett. **2017**, 58, 474-477.

[2] Y. Hu, J. Zhang, Y.-Z. Lv, X.-H. Huang, S.-l. Hu, Spectrochim. Acta - A: Mol. Biomol. Spectrosc. **2016**, 157, 164-169.

[3] M. S. Kim, J. M. Jung , J. H. Kang , H. M. Ahn , P.-G. Kim, C. Kim ,Tetrahedron **2017**, 73, 4750-4757.

[4] H. Liu, S. Cui, F. Shi, S. Pu , Dyes Pigm. **2019**, 161, 34-43.

[5] P. Roy, S. Das, K. Aich, S. Gharami, L. Patra, T. K. Mondal , J. Indian Chem. Soc. **2017**, 94, 755-760.

[6] M. Pannipara, A. G. A. Sehemi, M. Assiri, A. Kalama , Opt. Mater. **2018**, 79, 255–258.

[7] P. A. Patil, S. Sehlangia, C. P. Pradeep , Sensors International 2021, 2, 100075.

[8] S.-M. Shi, Q. Li, S.-L. Hu, J. Chem. Res. **2019**, 43, 426–430.

[9] H. Tavallali, G. Deilamy-Rad, M. A. Karimi, E. Rahimy, Anal. Biochem. **2019**, 583, 113376.
[10] Y. Zhang, Y.-T. Wang, X.-X. Kang, M. Ge, H.-Y. Feng, J. Han, D.-H. Wang, D.-Z. Zhao, J. Photochem. Photobiol. A: Chem. **2018**, 356, 652-660.
[11] M. Zhao, Y. Zhang, X. Zheng, Z. Li, S. Xu , Inorg. Chem. Commun. **2020**, 121, 108198.